Virtual Plasma Equipment Model: A Tool for Investigating Feedback Control in Plasma Processing Equipment

Shahid Rauf, *Member, IEEE*, and Mark J. Kushner, *Fellow, IEEE*

***Abstract*—As microelectronics device feature sizes continue to shrink and wafers continue to increase in size, it is necessary to have tighter tolerances during the fabrication process to maintain high yields. Feedback control has, therefore, become an important issue in plasma processing equipment design. Comprehensive plasma equipment models linked to control algorithms would greatly aid in the investigation and optimal selection of control strategies. This paper reports on a numerical plasma simulation tool, the Virtual Plasma Equipment Model (VPEM), which addresses this need to test feedback control strategies and algorithms on plasma processing equipment. The VPEM is an extension of the Hybrid Plasma Equipment Model which has been augmented by sensors and actuators, linked together through a programmable controller. The sensors emulate experimental measurements of species densities, fluxes, and energies, while the actuators change process parameters such as pressure, inductive power, capacitive power, electrode voltages, and mole fraction of gases. Controllers were designed using a response surface based methodology. Results are presented from studies in which these controllers were used to compensate for a leak of N_2 into an Ar discharge, to stably control drifts in process parameters such as pressure and power in Ar and Ar/Cl_2, and to nullify the effects of long term changes in wall conditions in Cl_2 containing plasmas. A new strategy for improving the ion energy flux uniformity in capacitively coupled discharges using feedback control techniques is also explored.**

I. Introduction

PLASMA processing (etching, deposition, cleaning) is one of the most important procedures employed for manufacturing of microelectronics devices [1]. Most of the plasma processing reactors now in the fabrication facilities operate in the open loop mode, where process parameters are set based on recipes and past experience with little, if any, real time feedback from the etching or deposition process per se. As the microelectronics feature sizes continue to shrink and wafers continue to increase in size, it is necessary to have tighter tolerances during the fabrication process to maintain high yield. This is particularly true for plasma processing steps. Feedback control has, therefore, recently become an important issue in plasma processing equipment design, and has motivated a number of investigations into its implementation [2]–[8]. The basic goal in these studies is to monitor, for example, etching or deposition rates using *in situ* diagnostics, and control process parameters that are more directly related to the measured quantities. The choice of control strategies is largely motivated by one's ability to measure the desired quantities. Considerable work is, therefore, also in progress to develop robust diagnostics [9]. The development of feedback control strategies has historically been largely empirical, based on experimentally observed correlations between sensor data and etch processes. The goal of the present research is to develop a computational tool that can be used for theoretically investigating feedback control strategies for plasma processing equipment, and to provide guidance for experimental tool development.

The most common approach to feedback control of plasma processing reactors makes use of statistical methods [2], [3]. Using data from experiments, response surfaces linking product parameters (such as etch rate) and controllable process parameters (such as gas pressure and power) are constructed. These models are then used to dynamically control etching and deposition processes. Rashap *et al.* [4] have investigated feedback control in a reactive ion etching (RIE) reactor using controllers designed through system identification techniques which utilize the systems response to step changes in actuators. Sarfaty *et al.* [5] used a two color laser interferometer in conjunction with proportional integral derivative (PID) controllers to control etch rate by means of rf bias voltage in a magnetically confined inductively coupled plasma (ICP). An alternate approach is the use of reduced order or phenomenological models for the plasma [6]. Neural networks have also been used for controlling etch processes [7]. While the above mentioned studies are primarily experimental, Ventzek *et al.* [8] theoretically investigated the feasibility of improving plasma uniformity at the wafer by controlling the antenna coil currents in an ICP source. This method has recently been demonstrated experimentally by Le *et al.* [10].

The computational tool we have developed to investigate feedback control is called the Virtual Plasma Equipment Model (VPEM). The VPEM is an extension of the Hybrid Plasma Equipment Model (HPEM) [11]–[13], a comprehensive plasma equipment simulation tool. To make the HPEM suitable for studying issues related to feedback control, we added sensor, actuator, and programmable controller modules. The sensor module emulates measurements of experimental

Manuscript received May 20, 1997; revised November 14, 1997. This work was supported by the Air Force Office of Scientific Research (F49620-95-1-0524), the National Institute of Standards and Technology, the National Science Foundation (ECS 9404133), the Semiconductor Research Corporation, and the University of Wisconsin ERC for Plasma Aided Manufacturing.

The authors are with the Department of Electrical and Computer Engineering, University of Illinois, Urbana, IL 61801 USA (e-mail: rauf@uigela.ece.uiuc.edu; mjk@uiuc.edu).

Publisher Item Identifier S 0894-6507(98)05889-8.

sensors. Some of the implemented sensors (and their experimental analogs) are spatially averaged densities (optical emission spectroscopy), ion flux to surfaces (ion energy analyzer) and plasma density (Langmuir probe). The actuator module changes process parameters that can be externally controlled in experiments such as inductively coupled power, applied voltage on electrodes, gas pressure, flow rate, and mole fraction of gases in the feed. The sensor and actuator modules are linked together through a programmable controller.

In this study, we used the VPEM to evaluate controller designs and test feedback control strategies in ICP and RIE systems. The controllers were designed using a response surface based technique. The design procedure consisted of constructing the response surfaces over the actuator parameter range of interest, fitting a polynomial to these response surfaces, and using their coefficients to develop a linearized model for system response. In practice, these controllers were found to be fairly robust against drifts in actuators and external disturbances. We considered Ar, Ar/N_2, and Ar/Cl_2 gas mixtures. In ICP reactors, the sensors we used were spatially averaged species density (which emulates experimental optical emission spectroscopy or microwave sensors) and ion flux to wafer (which, in ion driven etch processes such as SiO_2, emulates etch rate). The actuators included inductive power, pressure and rf voltage on the biased electrode. It was found that one and two variable controllers were able to compensate for perturbations caused by small gas leaks and modification in reactor surface, and control up to 20% drifts in actuators. In the RIE reactor, we demonstrated the capability of designing controllers by investigating a technique for improving the uniformity of wafer-impinging ion energy flux. In this technique, the powered electrode of the RIE reactor is split into two, and the voltage on the two segments is controlled independently.

The VPEM is described in Section II. In Section III, we explain the controller design procedure. Results from the VPEM are presented in Section IV, and concluding remarks are in Section V.

II. Description of the Virtual Plasma Equipment Model

In this section, we describe the Virtual Plasma Equipment Model (VPEM). The general structure of the VPEM is shown in Fig. 1(a). The VPEM uses the HPEM for simulating the plasma equipment. The HPEM is a comprehensive plasma equipment simulator that has been developed at the University of Illinois [11]–[15]. Since the HPEM has been described in detail in several previous publications, it is only briefly discussed here. The HPEM consists of three coupled modules. The first module computes the inductively coupled electromagnetic fields and also simulates the circuitry supplying power to the inductive coils. The electromagnetic fields are passed to the second module which simulates electron energy transport. Electron energy transport can be simulated in a number of ways including a Monte Carlo simulation and solution of the electron energy equation coupled with the Boltzmann equation to provide rate coefficients. The second module computes

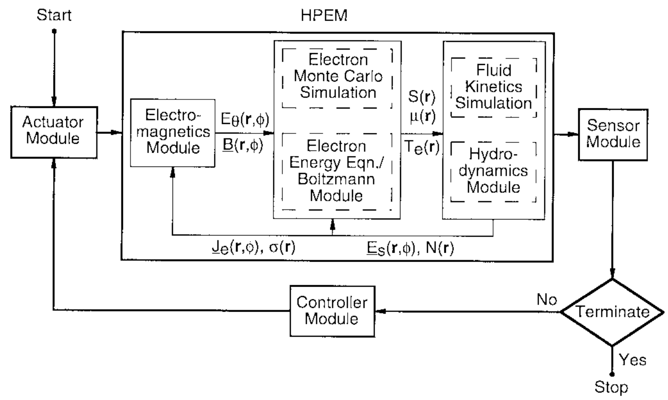

(a)

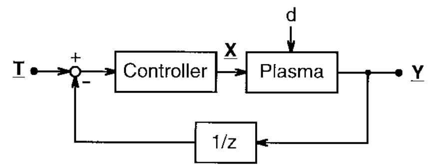

(b)

Fig. 1. (a) A schematic diagram of the Virtual Plasma Equipment Model (VPEM). The VPEM consists of an actuator module, a sensor module, a controller module, and the Hybrid Plasma Equipment Model (HPEM). The HPEM simulates the plasma and it is the major computational tool in the VPEM. The other three modules interconnect HPEM's inputs and outputs into a feedback control loop. (b) A block diagram of the plasma chamber along with the controller. d is an external disturbance that modifies the plasma system. $1/z$ designates a delay of one controller time step.

the electron energy distribution function, electron temperature, source functions for various electron impact reactions, and electron transport coefficients. Using this information, the third module simulates ions, electrons, and neutral species transport in the plasma, and also generates the electrostatic fields. The electrostatic field and species densities computed by the third module are passed back to the first two modules, which completes the loop. The HPEM iterates the three modules until quasisteady-state plasma conditions are obtained.

To make the HPEM suitable for investigating feedback control problems, three modules were added. In the actuator module, process parameters including inductively coupled power, capacitively coupled power, voltage on electrodes, gas pressure, gas flow rate, mole fraction of gases in the feed, operating frequency, and relative currents on inductive coils can be adjusted. In the sensor module, the output of the HPEM is used to emulate quantities that are ideally measured by experimental sensors. The sensors (and their experimental analog) include the following for any species or combination of species:

1) density at a given point (rf probes and optical diagnostics);
2) spatially averaged density in the reactor (optical and microwave diagnostics);
3) spatially averaged density within a cone (optical diagnostics);
4) flux at a given point in a given direction (mass spectrometer),
5) total reactant flux impinging on the wafer (etch rate);

6) total flux at the pump port (residual gas analyzer);
7) energy flux at a given point on the wafer (etch rate).

The sensor and actuator modules are linked through a controller module.

In a typical VPEM simulation, the user sets up a HPEM simulation and, in addition, specifies the sensors and actuators. The HPEM then computes the quasisteady-state plasma conditions. This information is used by the sensor module to emulate sensor data, which is checked against a user specified termination condition. If that condition is not satisfied, sensor data is passed to the controller module. The controller module computes how much the actuators need to be adjusted, and passes this information to the actuator module. The actuator module adjusts the actuators and reruns the HPEM simulation. This procedure is repeated until the termination condition is satisfied.

It has been assumed that the sampling time of the controller is much longer than the equilibration time of the plasma following perturbations to its operating conditions. Therefore, in between actuator adjustments, the plasma reaches quasisteady-state conditions. This assumption is strictly valid for a run-to-run control scenario. For real time control, it imposes a fundamental limitation on the maximum controller frequency that could be used. A study by Yang *et al.* [16] indicates that the disturbances produced in the plasmas of interest due to small step changes in actuators (such as power deposition) are generally stabilized in a few milliseconds. For changes in flow conditions (such as composition of the feedstock gases or flow rate), the equilibration time is approximately a residence time of the gas, which for the systems of interest is 10 s to a few hundred milliseconds. It therefore appears safe to assume that the results of the present study will be valid if the controller time step is 0.1 s or larger. It does, however, need to be explored in more detail as to what is the minimum time step size beyond which dynamic models, as opposed to the present static one, become necessary.

III. Controller Design

In past studies, a variety of approaches have been used to design feedback controllers. Rashap *et al.* [4] used an experimental system identification technique which utilized the response of the plasma system to step changes in actuators. Mozumder and Barna [2] developed response surface based models and determined optimal actuator settings based on them. Ventzek *et al.* [8] used a proportional integral derivative (PID) controller whose gain was estimated using the step response of the plasma system. Rietman *et al.* [7] used neural networks to control etching processes. We have kept the structure of the controller module general enough that all of these types of controllers can be implemented. In the feedback control problems we investigate in this paper, we used a response surface based technique to design the controllers. Since the basic control scheme in the VPEM is more akin to run-to-run control, this approach was found to be adequate for designing robust controllers. The controller design technique is described below.

The first step in the controller design procedure is to decide which sensors, actuators and range in actuator parameters are to be used for a given problem. Using this information, one runs HPEM simulations at selected points within the actuator parameter range and constructs response surfaces of sensor outputs as a function of actuator settings. We used design of experiment techniques to reduce the number of simulations that must be performed to make the response surfaces. Specifically, a commercial design of experiment software, Echip© [17], was used to specify points where sensor data is needed. For controller design, the relevant information that is extracted from these response surfaces is the least mean square polynomial approximations linking the sensors and actuators. In our studies, we found that a quadratic polynomial was adequate for designing stable controllers. We will, therefore, restrict our attention to a quadratic polynomial in the following discussion. If the actuator parameter range of interest is broader or the system is strongly nonlinear, this procedure can be extended to handle polynomials of higher order. For a n-actuator n-sensor system, these polynomials have the form

$$\begin{aligned} y_j = c_j &+ \sum_{k=1}^{n} a_{jk}(x_k - x_{k0}) \\ &+ \sum_{k=1}^{n}\sum_{l=1}^{n} b_{jkl}(x_k - x_{k0})(x_l - x_{l0}) \end{aligned} \tag{1}$$

where $j = 1, 2, \cdots, n$. y_j are the outputs (sensors), x_k are the inputs (actuators), x_{k0} are the center point within the range of x_j, and c_j, a_{jk}, and b_{jkl} are constants obtained from the response surfaces.

We studied three type of control problems using the VPEM: 1) control of drifts in actuators, 2) compensation for change in parameters other than actuators, and 3) adjustment of actuators so that the sensors approach some pre-specified values. Although the implementation details vary, the basic goal in all these problems was to adjust the actuators $\underline{X} = [x_1, x_2, \cdots, x_n]^T$ so that the sensor signal $\underline{Y} = [y_1, y_2, \cdots, y_n]^T$ can be made to approach a desired target $\underline{T} = [t_1, t_2, \cdots, t_n]^T$ [see Fig. 1(b)]. To determine how much the actuators need to be adjusted in a given situation, we consider a small change δx_k in actuators in (1). This will modify the sensor outputs to $y_j + \delta y_j$. Assuming that $\delta x_k \ll x_k$, we can differentiate (1), linearize the resulting equation and write it in matrix form as

$$\underline{\delta X} = \underline{\underline{A}}^{-1} \cdot \underline{\delta Y} \tag{2}$$

where $\underline{\delta Y} = [\delta y_1, \delta y_2, \cdots, \delta y_n]^T$, $\underline{\delta X} = [\delta x_1, \delta x_2, \cdots, \delta x_n]^T$ and $\underline{\underline{A}}$ is an $n \times n$ matrix with elements

$$A_{jk} = a_{jk} + \sum_{l=1}^{n} (b_{jkl} + b_{jlk})(x_l - x_{l0}). \tag{3}$$

Setting $\underline{\delta Y} = \underline{T} - \underline{Y}_m$ and $\underline{\delta X} = \underline{X}_{m+1} - \underline{X}_m$, where the subscript m denotes the current settings and $m+1$ denotes the new values, we can write (2) as

$$\underline{X}_{m+1} = \underline{X}_m + \underline{\underline{B}} \cdot \underline{\underline{A}}^{-1} \cdot (\underline{T} - \underline{Y}_m). \tag{4}$$

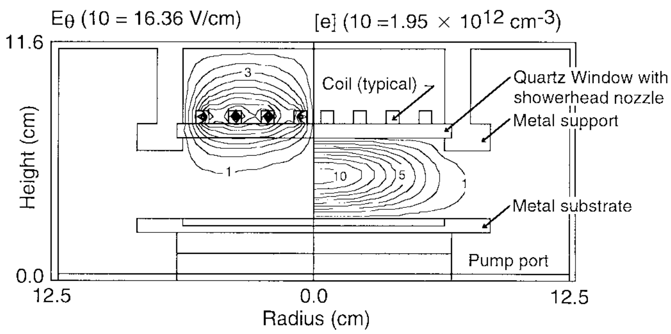

Fig. 2. The electric field amplitude and plasma density profiles in the ICP reactor. The operating conditions are: argon, 400 W inductive power, 20 mtorr gas pressure, no rf bias voltage on the lower electrode, and 10 sccm gas flow rate. All the ICP control studies in this paper were conducted with this reactor configuration.

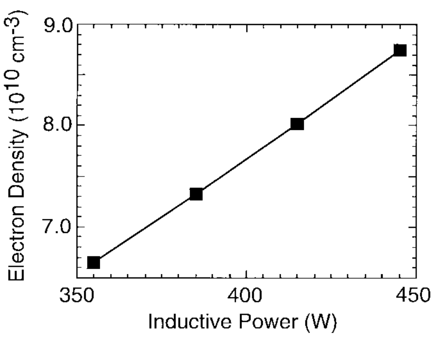

Fig. 3. One variable response surface for an ICP reactor with argon (17 mtorr). The actuator is inductive power deposition and the sensor is average electron density.

We multiplied $\underline{\underline{A}}^{-1}$ by an $n \times n$ diagonal matrix $\underline{\underline{B}}$ so that the actuator gains can be individually changed to improve stability. We use (4) for implementing the controllers in the VPEM.

IV. Feedback Control of Plasmas

We used the VPEM to study a number of feedback control problems in ICP and RIE reactors. In these problems, we investigated whether controllers designed using the technique described in Section III can compensate for drifts in process parameters such as power and pressure, changes in reactor wall conditions, and gas leaks. We also explored a new technique for improving the uniformity of ion energy flux at the wafer.

To illustrate the use of the VPEM, we first consider a one variable controller in an ICP reactor using argon powered at 13.56 MHz. The reactor is a modified form of the inductively coupled Gaseous Electronics Conference (GEC) reference cell [18]. The plasma density and electric field amplitude are shown in Fig. 2 for typical conditions (argon, 400 W, 20 mtorr, 10 sccm, no substrate bias). We chose inductive power to be the actuator and the sensor was spatially averaged electron density as might be measured by microwave interferometry. The gas pressure was kept constant at 17 mtorr and the lower electrode was not biased. Simulations were run at several powers between 350 and 450 W to construct the response surface, which is shown in Fig. 3. As expected, higher power deposition produces a higher plasma density in an almost linear fashion. Using this response surface, a controller was designed

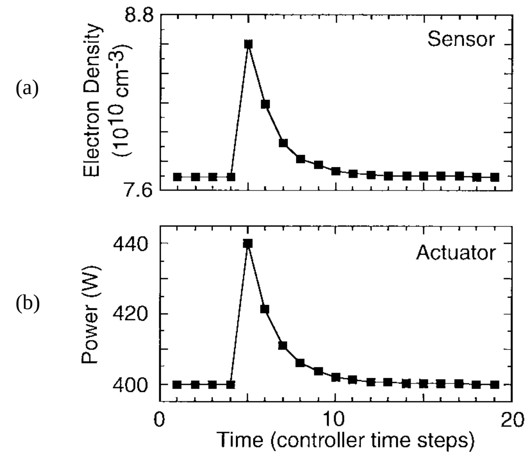

Fig. 4. Sensor and actuator time history for a control case in which the controller compensates for a drift in the actuator for an argon ICP tool (17 mtorr). The sensor is spatially averaged electron density and the actuator is inductive power. The controller gain is multiplied by 0.5 [$B_{11} = 0.5$ in (4)].

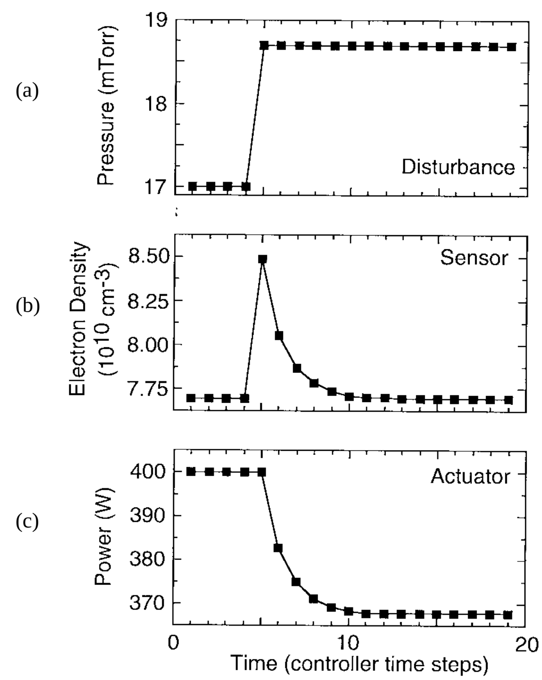

Fig. 5. Sensor, actuator, and disturbance time history for a control case in which the controller compensates for an external disturbance for an argon ICP tool. The sensor is spatially averaged electron density, the actuator is inductive power and gas pressure is the external disturbance. The controller gain is multiplied by 0.5 [$B_{11} = 0.5$ in (4)].

that would keep the sensor output at a given value. Results from two control cases that utilize this controller are shown in Figs. 4 and 5. In the first example (Fig. 4), we increase the inductive power deposition (actuator) by 10% at $T = 5$. There is a corresponding increase in the sensor output as the plasma density increases in response to the change in power. The controller is then used to adjust the actuator to nullify the change in the sensor signal. As the results illustrate, the controller is able to bring the power and spatially averaged electron density back to their original values, and keep them there. The gain in the controller was multiplied by 0.5 to increase the controller response time.

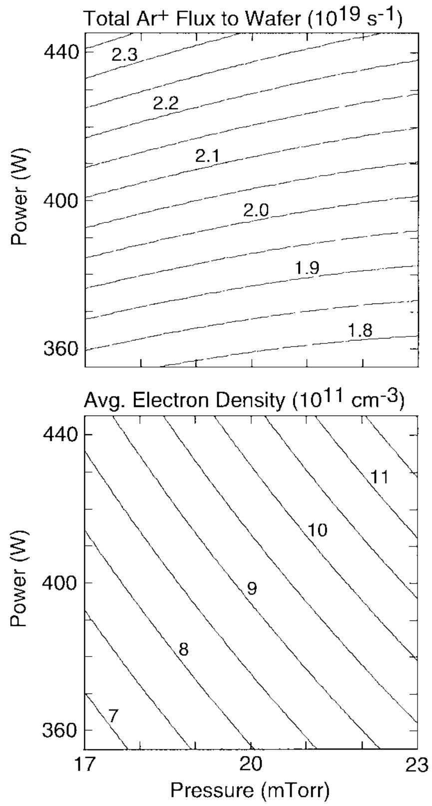

Fig. 6. The response surfaces for a two-sensor two-actuator control case in an ICP reactor with Ar. The sensors are spatially averaged plasma density and total flux of Ar^+ ions to the wafer. The actuators are inductive power and gas pressure.

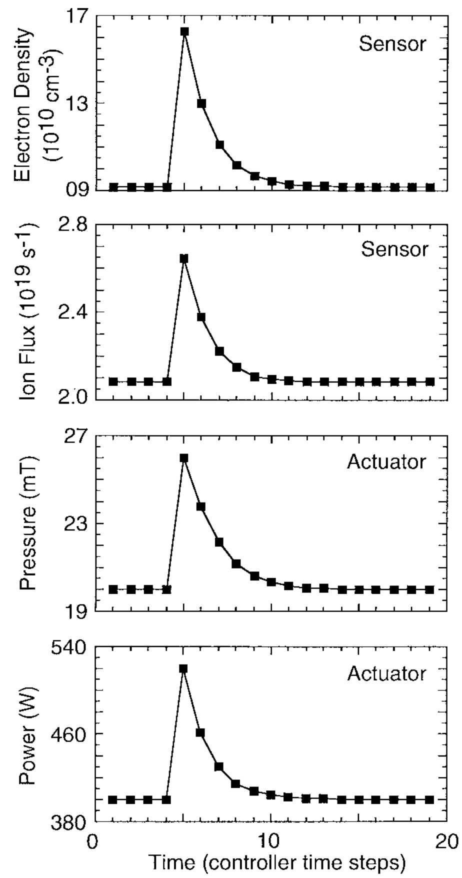

Fig. 7. Sensor and actuator time history for an Ar ICP tool in which the controller nullifies a 30% increase in both actuators. The sensors are spatially averaged electron density and total flux of Ar^+ ions to the wafer. The actuators are inductive power and pressure. Controller gains are multiplied by 0.5 [$B_{11} = B_{22} = 0.5$ in (4)].

A more interesting case in shown in Fig. 5 where we increase the pressure by 10%. Since pressure is not an actuator, the controller is not specifically designed to handle variations in pressure. However, assuming that small changes in pressure do not perturb the response of the system significantly, the controller should work in this situation as well. This is verified by the results in Fig. 5 where the controller adjusts the power to bring the sensor signal (electron density) back to its original value. In this parameter regime, the plasma density increases with increasing pressure at constant power deposition since the rate of loss by diffusion is inversely proportional to pressure. The controller's response to an increase in pressure, which increases plasma density, was to decrease the power to compensate. This particular result is sensitive to the details of electron–ion recombination. At higher gas pressures where volumetric recombination dominates, the plasma density does not scale linearly with power deposition, and therefore a higher order controller may be required.

We next consider the same plasma system but use a two variable controller. The actuators are inductive power deposition and gas pressure. The sensors are spatially averaged electron density and total flux of Ar^+ ions to the wafer to emulate the etch rate of an ion driven process. The resulting response surfaces of sensor outputs as a function of pressure and power are shown in Fig. 6. Both plasma density and Ar^+ flux to the wafer increase with increasing power deposition. In this parameter regime, plasma density increases with increasing pressure due to the lower rate of loss by diffusion. Ar^+ ion flux to the wafer, on the other hand, decreases slightly as gas pressure is increased at constant power. One can attribute this to a higher collision rate at larger pressures, which reduces the mean ion speed and hence flux. The controller obtained from this response surface was found to be robust against changes in actuators. For example, results from a control case in which both pressure and power are increased by 30% are shown in Fig 7. When gas pressure and inductive power are increased, both plasma density and Ar^+ ion flux to the wafer increase in accordance with predictions by the response surfaces. To nullify this large change, the controller decreases pressure and power until the sensors come back to their original values. To improve stability, we have again multiplied the controller gain by 0.5, which also increases the response time of the controller.

It is well known that addition of even small amount of molecular or attaching gases to rare gas discharges can significantly change the plasma parameters. It would be useful if feedback controllers can compensate for this type of disturbance which might occur as a result of a chamber gas leak. In the next example, we consider a case in which there is a leak at the gas inlet and small amount of N_2 flows into the ICP reactor intended to operate in pure argon. The gas leak changes the spatially averaged electron density and flux of Ar^+

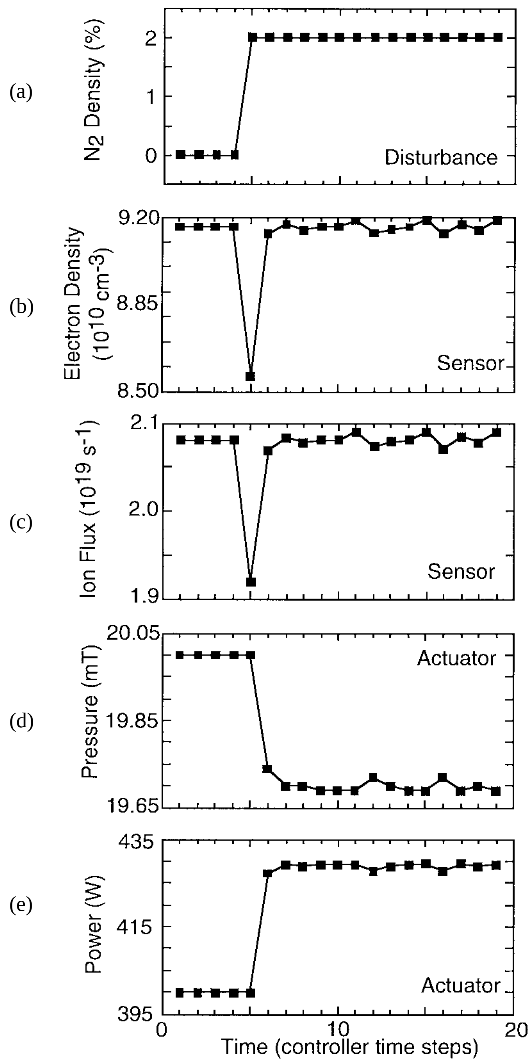

Fig. 8. Sensor, actuator, and disturbance time history for a control case in an ICP tool for which the controller compensates for a leak at the gas inlet. The sensors are spatially averaged electron density and total flux of Ar^+ ions to the wafer. The actuators are inductive power and gas pressure. The external disturbance is a leak of N_2 into the reactor operating in Ar.

ions to the wafer. We used the 2-sensor 2-actuator controller described above to compensate for the N_2 leak and the results are shown in Fig. 8. When N_2 was leaked into the reactor while keeping the power deposition constant, some power was diverted toward nonionizing excitation of N_2 thereby reducing the electron temperature. This reduced the power available for ionization of Ar, and led to a smaller electron density and smaller Ar^+ ion flux to the wafer. The controller responded to the reduced sensor outputs by increasing the inductive power, which brought both sensor signals close to their original values. The pressure is also reduced slightly to compensate for the over or undershooting that might have occurred if only inductive power would have been adjusted. The small oscillations in the steady-state are a consequence of the fact that the controller is operating in a system (Ar/N_2) that is different from the one it was designed for (pure Ar). The response surface obtained for the pure Ar case captures the qualitative behavior but is not quantitatively accurate. At every time step, it either under or over-estimates the actuator change, which produces the oscillations. One can reduce the oscillation amplitude by decreasing the controller gain. This will, however, adversely effect controller response time. The ion flux to the substrate will contain some small percentage of N_2^+ when nitrogen is leaked into the cell, whereas our sensor, emulating a mass selective ion energy analyzer, measures only the Ar^+ flux. The response of the controller will be different if the total ion flux is measured, however that difference is small for these conditions and do not change the trends we have observed.

When reactive gases are used in plasma processing systems, the wall conditions may change over time due to passivation or polymer buildup. This can produce long term drifts in plasma characteristics by appreciably changing the reactive sticking coefficient of radical species on the reactor walls. One such example is the reaction Cl $\rightarrow$ wall $\rightarrow$ 0.5 Cl_2. A long term increase in the coefficient for this process increases the Cl_2 density, decreases the Cl density and increases the electronegativity of the plasma due to increased attachment to Cl_2 [19]. A useful application of feedback controllers would be to compensate for this change in reactive sticking coefficient. In the next case, we consider a 10% mixture of Cl_2 in Ar. The reactor is the same as shown in Fig. 3. The lower electrode is, however, biased with an rf voltage. To design the controller, we chose inductive power and bias voltage on the electrode as the actuators. Although the bias voltage does not appreciably change the ionization rate, the uniformity of ion flux to the substrate can be affected, as well as the mole fraction of any given species [12]. The sensors were spatially averaged electron density and total Cl^+ flux to the wafer. The choice of sensor for any particular control case depends on theoretical or empirical correlations between measurable quantities and the desired product, etch rate for example. Although it is more difficult to experimentally measure only the Cl^+ flux, as opposed to the ion flux, we chose this particular sensor because it is more correlated with the disturbance that the total ion flux.

To simulate a change in wall conditions, we increased the sticking coefficient of Cl at the reactor walls which formed Cl_2 from 0.0025 to 0.01 at $T = 5$. The results for this change in coefficient are shown in Fig. 9. An increase in the sticking coefficient resulted in more Cl_2 in the reactor, which reduced the electron density due to dissociative attachment. The decrease in electron density led to a smaller Cl^+ concentration in the reactor and smaller Cl^+ flux to the wafer. Since the Cl atom density also decreases due to the increase in wall recombination, there is less Cl to ionize. The controller responded to the change in sensor signals by increasing inductive power and reducing rf bias voltage. This brought both sensor signals back to their original values. The rf bias voltage increased since, in this parameter range, Cl^+ flux to the wafer increases slightly with decreasing rf bias voltage due to differences in mobility between Cl^+, Ar^+, and Cl_2^+. A second increase in sticking coefficient (0.01 to 0.04) produces a similar response in the actuators.

Another parameter that may drift over time in the Ar/Cl_2 system is gas pressure. In Fig. 10, we use the controller

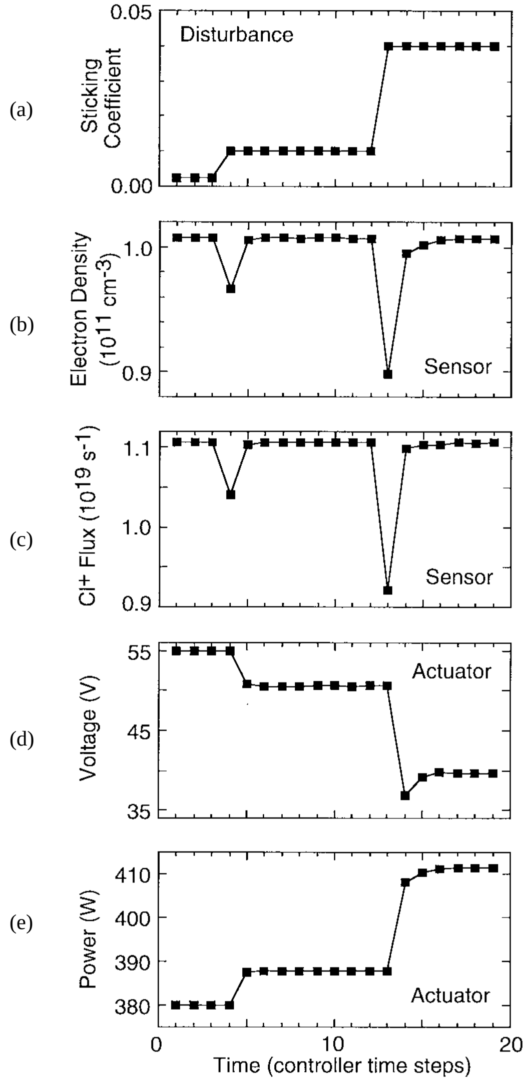

Fig. 9. Sensor, actuator, and disturbance time history for a control case in an ICP tool for which the controller compensates for a change of the sticking coefficient of Cl atoms on the reactor walls. The sensors are spatially averaged electron density and total flux of Cl^+ ions to the wafer. The actuators are inductive power and bias voltage on the lower electrode. The gas mixture is $Ar/Cl_2 = 90/10$ at 27 mtorr.

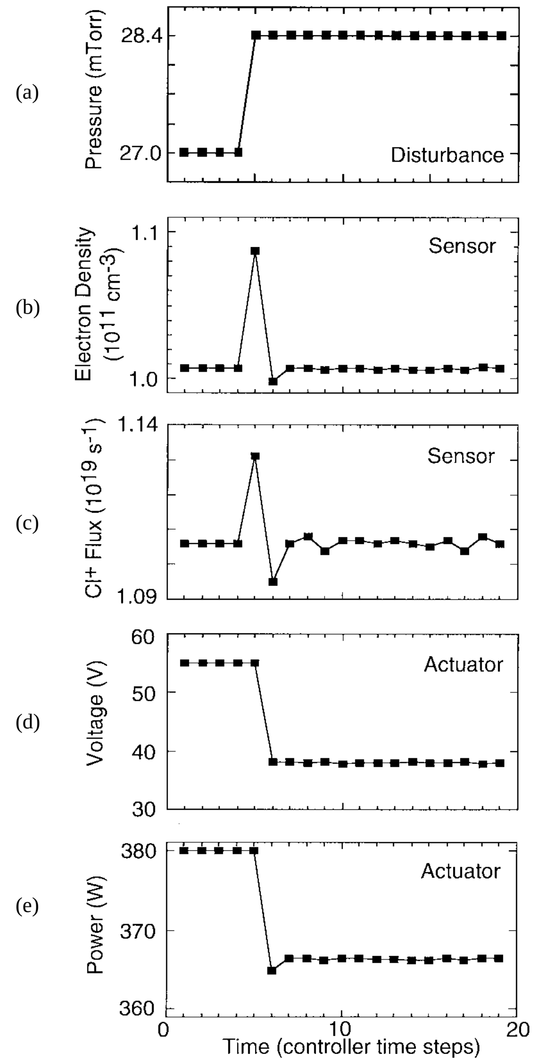

Fig. 10. Sensor, actuator, and disturbance time history for an ICP tool in which the controller compensates for a change in the gas pressure. The sensors are spatially averaged electron density and total flux of Cl^+ ions to the wafer. The actuators are inductive power and voltage on the lower electrode. The gas mixture is $Ar/Cl_2 = 90/10$.

described for the last example to compensate for a 5% increase in pressure. As for the pure argon system, the electron density increased when pressure was increased. An increase in the density of electrons also resulted in a larger flux of Cl^+ ions to the wafer. To compensate for the change in sensor signals, the controller decreased the inductive power and rf bias voltage. The Cl^+ flux, however, is more sensitive to process parameters at the higher pressures, and therefore oscillates slightly about the set point.

The problems we discussed in the context of ICP reactors can occur in RIE reactors as well. Using similar algorithms, we were successful in designing stable controllers that could control external disturbances and changes in actuators in RIE reactors. These results will, however, not be described here. We instead demonstrate how the VPEM (or similar computational tools) can be used to design controllers for improving the ion energy flux uniformity at the wafer in RIE reactors. The basis of this controller is the observation by Ding *et al.* [20] that the energy flux to the wafer is the dominant factor in determining etch rate in many fluorocarbon oxide etch systems. The reactor we used is a parallel plate capacitively coupled discharge in which the powered electrode has been split into two annular rings as shown in Fig. 11. The voltages applied to the two electrode segments can be separately controlled. Typical plasma parameters are shown in Fig. 11 for Ar at 100 mtorr, 10 sccm gas flow, and 13.56 MHz bias frequency. The plasma density is maximum near the edge of the electrode, an effect attributed to electric field enhancement [21]. In designing the two-actuator two-sensor controller, we chose the voltage applied to the two electrodes to be the actuators. The sensors were placed on top of the substrate at the mid point of the annuli, and they measured a quantity proportional to the ion energy flux. The ion energy flux at both sensors was found to increase when voltage was increased and, as expected, correlate well with the voltage

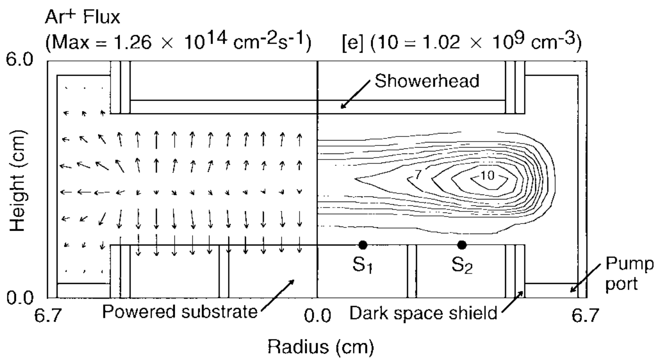

Fig. 11. Ar^+ flux and plasma density in the reactive ion etching reactor. The operating conditions are: Ar, 100 mtorr, 130 V applied to both inner and out electrodes, and 10 sccm gas flow. S_1 and S_2 are the locations of the two sensors.

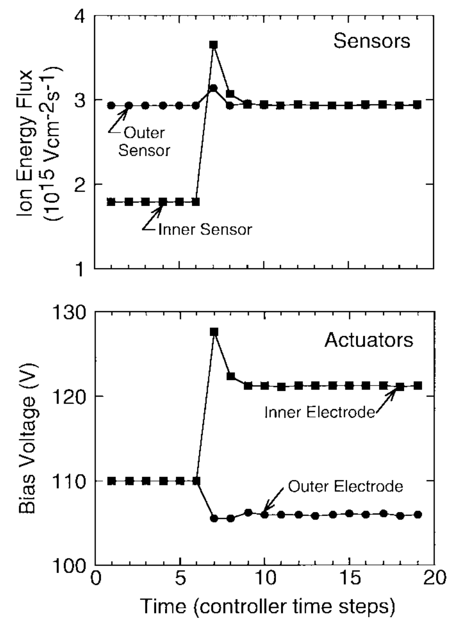

Fig. 12. Sensor and actuator time history where the controller tries to improve the uniformity of ion energy flux at the substrate in the split electrode RIE reactor (Fig. 11) with Ar. The actuators are bias voltages on the two electrodes. The sensors measure a quantity proportional to ion energy flux at two points on the wafer.

at the corresponding electrode. There was, however, a weak dependence on the voltage of the other electrode as well since radial transport of ions generated above one annulus can produce an ion flux on the other annulus. To quantify the uniformity of the ion flux to the substrate, we define $U = (E_{\max} - E_{\min})/(E_{\max} + E_{\min})$ [8] where $E_{\max}$ and $E_{\min}$ are the maximum and minimum ion energy flux onto the substrate. Smaller U means better uniformity.

For the problem of interest, we designed a new controller which would adjust the voltage on the two electrodes with the goal of equating the ion energy flux at the two sensors. The results are shown in Fig. 12. Initially, the voltage on the two electrodes are kept equal. The resulting ion energy flux is larger on the outer annulus due to the higher ion density near the edge of the electrode, producing a uniformity of $U = 0.27$. After the controller is turned on, the voltages are adjusted so that the two sensor signals become nearly equal. The voltage on the outer electrode is decreased to compensate for the electric field enhancement which produces a higher ion density. The voltage on the inner electrode increases to locally produce more ions which are more energetic. With the controller on, the uniformity improves from $U = 0.27$ to $U = 0.05$.

The control solutions which we have obtained in this study are not necessarily unique. There may be alternate paths from the perturbed conditions to the desired set points which are not captured by the VPEM since we have linearized the response surface in the controller algorithm. We see consequences of this situation if we greatly perturb the system by, for example, disturbing a system by 30% from its nominal value. Following such a large perturbation, the linearized controller may not be able to recover the set point conditions since the restoring path on the response surface has nonlinear elements. Since the control problems of interest typically address smaller perturbations in operating conditions, the nonunique nature of the solution is not terribly limiting.

V. Concluding Remarks

In this paper, we described a computational plasma simulation tool, the Virtual Plasma Equipment Model (VPEM), that was used to investigate feedback control problems in plasma processing equipment. The VPEM uses a detailed plasma equipment model, HPEM, for simulating the plasma. The input and output of the HPEM are linked through a sensor module, a controller module, and an actuator module. A large number of actuators and sensors have been implemented which makes VPEM a versatile tool for evaluating feedback control strategies and controller designs.

We used the VPEM to study a number of feedback control problems in ICP and RIE reactors. The controller in these studies were designed using a response surface based methodology. Results from the simulation suggest strategies whereby drifts in process parameters such as pressure and inductive power deposition can be controlled, and gas leaks and changes in reactor wall conditions can be compensated. We also investigated a technique for improving the ion energy flux uniformity at the wafer. This technique uses a split powered electrode RIE reactor in which the voltage on the two segments is modified using a feedback controller.

The controllers in the present study have been designed using static plasma models which appear suitable for low controller frequencies typically used in practice. Control frequencies commensurate with the plasma equilibration time scales will, however, necessitate the use of dynamic models. This is computationally a very challenging problem which may require less comprehensive plasma models to be tractable.

Acknowledgment

The authors would like to thank P. Khargonekar, F. Terry, and E. Hamby for useful discussions.

REFERENCES

[1] D. M. Manos and D. L. Flamm, Eds., *Plasma Etching: An Introduction.* New York: Academic, 1989.

[2] P. K. Mozumder and G. G. Barna, "Statistical feedback control of a plasma etch process," *IEEE Trans. Semiconduct. Manufact.,* vol. 7, pp. 1–11, Feb. 1994.

[3] C. J. Spanos, H. F. Guo, A. Miller, and J. Levine-Parrill, "Real-time statistical process control using tool data," *IEEE Trans. Semiconduct. Manufact.,* vol. 5, pp. 308–318, 1992.

[4] B. A. Rashap, M. Elta, H. Etemad, J. P. Fournier, J. S. Freudenberg, M. D. Giles, J. W. Grizzle, P. T. Kabamba, P. P. Khargonekar, S. Lafortune, S. M. Meerkov, J. R. Moyne, D. Teneketzis, and F. L. Terry, Jr., "Control of semiconductor manufacturing equipment: Real-time feedback control of a reactive ion etcher," *IEEE Trans. Semiconduct. Manufact.,* vol. 8, pp. 286–297, 1995.

[5] M. Sarfaty, R. Breun, N. Hershkowitz, C. Baum, K. Nagpal, T. Vincent, and P. P. Khargonekar, "Real-time control of etch rate and selectivity using two color laser interferometry," in *Conf. Rec. 1996 IEEE Int. Conf. Plasma Science,* 1996, p. 281.

[6] M. Chandok, P. D. Hanish, and J. W. Grizzle, "Phenomenological modeling for real-time feedback control of RIE," in *Proc. 187th Meeting Electrochem. Soc. Process Control, Diagnostics and Modeling in Semiconductor Manufacturing,* M. Meyyappan, D. Economou, and S. W. Butler, Eds., 1995, vol. 95-3.

[7] E. A. Rietman, R. C. Frye, E. R. Lory, and T. R. Harry, "Active neural network control of wafer attributes in a plasma etch process," *J. Vac. Sci. Technol. B,* vol. 11, pp. 1314–1316, 1993.

[8] P. L. G. Ventzek, N. Yamada, Y. Sakai, H. Tagashira, and K. Kitamori, "Simulation of real-time control of two-dimensional features in inductively coupled plasma sources for etching applications," *J. Vac. Sci. Technol. A,* vol. 13, pp. 2456–2463, 1995.

[9] T. E. Benson, L. I. Kamlet, S. M. Ruegsegger, C. K. Hanish, P. D. Hanish, B. A. Rashap, P. Klimecky, J. S. Freudenberg, J. W. Grizzle, P. P. Khargonekar, F. L. Terry, Jr., and B. Barney, "Sensor systems for real-time feedback control of reactive ion etching," *J. Vac. Sci. Technol. B,* vol. 14, pp. 483–488, 1996.

[10] M. S. Le, D. S. Boning, and H. H. Sawin, "Run by run uniformity control on a dual coil transformer coupled plasma reactor with full wafer interferometry," in *Abstr. 43rd Nat. Symp. Amer. Vacuum Soc.,* 1996, p. 29.

[11] W. Z. Collison and M. J. Kushner, "Ion drag effects in inductively coupled plasmas for etching," *Appl. Phys. Lett.,* vol. 68, pp. 903–905, 1996.

[12] M. J. Grapperhaus and M. J. Kushner, "A semi-analytic sheath model integrated into a 2-dimensional model for radio frequency biased, inductively coupled plasma etching reactors," *J. Appl. Phys.,* vol. 81, pp. 569–577, 1997.

[13] P. L. G. Ventzek, M. Grapperhaus, and M. J. Kushner, "Investigation of electron source and ion flux uniformity in high plasma density inductively coupled etching tools using two-dimensional modeling," *J. Vac. Sci. Technol. B,* vol. 12, pp. 3118–3137, 1994.

[14] M. J. Kushner, W. Z. Collison, M. Grapperhaus, J. P. Holland, and M. S. Barnes, "A three-dimensional model for inductively coupled plasma etching reactors: Azimuthal symmetry, coil properties, and comparison to experiments," *J. Appl. Phys.,* vol. 80, pp. 1337–1344, 1996.

[15] S. Rauf and M. J. Kushner, "A model for noncollisional heating in inductively coupled plasma processing reactors," *J. App. Phys.,* vol. 81, pp. 5966–5974, 1997.

[16] J. Yang, P. L. G. Ventzek, Y. Sakai, K. Kitamori, H. Tagashira, and M. Meyyappan, "Step and pulsed responses of RF discharges," *Bull. Amer. Phys. Soc.,* vol. 42, p. 1703, 1997.

[17] *Echip User's Guide.* Hockessin, DE: Echip Inc., 1994.

[18] P. A. Miller, G. A. Hebner, K. E. Greenberg, P. D. Pochan, and B. P. Aragon, "An inductively coupled plasma source for the gaseous electronics conference RF reference cell," *J. Res. Nat. Inst. Stand. Technol.,* vol. 100, pp. 427–439, 1995.

[19] S. C. Deshmukh and D. Economou, "Factors affecting the Cl atom density in a Cl_2 discharge," *J. Appl. Phys.,* vol. 72, pp. 4597–4607, 1992.

[20] J. Ding, J.-S. Jeng, G.-H. Kim, H. L. Maynard, J. S. Hamers, and N. Hershkowitz, "Etching rate characterization of SiO_2 and Si using ion energy flux and atomic fluorine density in a $CF_4/O_2/Ar$ electron cyclotron resonance plasma," *J. Vac. Sci. Technol. A,* vol. 11, pp. 1283–1288, 1993.

[21] D. P. Lymberopoulos and D. J. Economou, "Two-dimensional self-consistent radio frequency plasma simulations relevant to the gaseous electronics conference RF reference cell," *J. Res. Nat. Inst. Stand. Technol.,* vol. 100, pp. 473–494, 1995.

Shahid Rauf (S'89–M'95) received the B.Sc. (Honors) degree from the University of Engineering and Technology, Lahore, Pakistan, in 1991, and the M.S. and Ph.D. degrees from the University of Wisconsin, Madison, WI, in 1992 and 1995, respectively, all in electrical engineering.

Since 1995, he has been with the Optical and Discharge Physics group at the University of Illinois, Urbana-Champaign. His present research focuses on the computational modeling of partially ionized plasmas and gas discharges. This work ranges in scope from the investigation of basic physics issues such as noncollisional electron heating to the development of computational tools for industrial plasma device modeling. In the past, he has conducted theoretical and experimental research on nonlinear plasma waves, magnetohydrodynamics, and high-power millimeter-wave antennas. His research has resulted in more than a dozen publications in international scientific journals and about 30 conference presentations.

Mark J. Kushner (S'74–M'79–SM'89–F'91) received the B.A. degree in astronomy and the B.S. degree in engineering from the University of California at Los Angeles in 1976, and the M.S. and Ph.D. degrees in applied physics from the California Institute of Technology, Pasadena, in 1977 and 1979, respectively, where he also was the Chaim Weissmann Postdoctoral Research Fellow.

He served on the technical staffs of Sandia National Laboratory, Lawrence Livermore National Laboratory, and Spectra Technology, Inc., prior to joining the Department of Electrical and Computer Engineering at the University of Illinois, Urbana-Champaign, in 1986, where he is now a Professor. He served as Assistant Dean of Academic Programs in the College of Engineering during 1994–1995. He has published more than 140 journal articles on topics related to plasma materials processing, amorphous thin films, gas and solid state lasers, pulse power plasmas, chemical lasers, and laser spectroscopy.

Dr. Kushner is a member of Phi Beta Kappa, Tau Beta Pi, Eta Kappa Nu, the American Vacuum Society, and the Materials Research Society. He is also a Member and Fellow of the American Physical Society and the Optical Society of America. He has served on the executive committees of the Gaseous Electronics Conference, the IEEE Technical Committee on Plasma Science and Applications, the AVS Plasma Science and Technology Division, the Gordon Conference on Plasma Chemistry, and the AVS Manufacturing Science and Technology Group. He is currently chair of the Gaseous Electronics Conference and the past chair of AVS Plasma Science and Technology Division. He is on the editorial board of *Plasma Sources Science and Technology* and the *Journal of Vacuum Science and Technology*, and serves as an Associate Editor of the IEEE TRANSACTIONS ON PLASMA SCIENCE.